International Journal of Research Findings in Engineering, Science and Technology | IJRFEST
p-ISSN: 2315-8417 | e-ISSN: 2489-0138
Volume 5, Number 1 May, 2023

Strength Optimization of Metakaolin-Based Geopolymer Concrete Modified with Metabentonite Using Response Surface Method

[1]A. Ahmed, [2]S. I. Bajahry, [3]I. Garba, [4]J. Abubakar, [5]A. Lawan, [6]A. Ocholi, & [7]J. M. Kaura
[1,2,3,4,5,6&7]Department of Civil Engineering,
Ahmadu Bello University, 5M35+H4V, 810106, Zaria, Kaduna

Article DOI: 10.48028/iiprds/ijrfest.v5.i1.03

Abstract

This paper, present the optimum compressive strength and characterization of Geopolymer Concrete (GP) produced by metakaolin and metabentonite. In the need for sustainable and eco-friendly concrete binding materials as alternative to ordinary Portland cement (OPC). Production of OPC required high amount of energy and emission of about 8% CO_2 to the atmosphere is significant to Green House Gasses (GHG). Utilization of alkaline activation materials in concrete may be a better alternative solution. In the Design of Experiment (DOE), randomized block factorial design of Response Surface Methodology (RSM) was used to optimize the strength. Metabentonite was replaced at 10, 20, 30, 40 and 50 wt.% of Metakaolin. The mixes were activated with 12 molar concentration (12M) of sodium hydroxide (NaOH) solutions and Na_2Si_3O/NaOH ratio of 1.5:1 at 50, 60 70, 80, and 90 % alkali doss (alkaline liquid-to-binder). The mix design properties such as binder ratio (metabentonite to metakaolin) and alkaline liquid-to-binder ratio were statistically employed as continuous (independent) variables to optimize the response factor (compressive strength). Compared to the control sample (metakaolin-based GPC), the metabentonite incorporated based GPC exhibited higher compressive strengths at up to 25 wt.% of metabentonite replacement. The models predicted the response of compressive strength with the variability of less than 5%. Moreover, the correlation between the experimental and optimized compressive strengths yielded high precision with 96.51% "R^2". Therefore, FTIR was used for characterization and the response models would be advantageous in optimization of mix design proportions to obtain the target compressive strength of GPC produced by metabentonite and metakaolin.

Keywords: *Alkaline Activation, Geopolymer Concrete, Compressive Strength, Modeling, Optimization*

Corresponding Author: **A. Ahmed**

Background to the Study

Geopolymer concrete utilizes Supplementary Cementitious Materials (SCMs) as the source materials for its production and it exhibits higher mechanical strength Bouaissi *et al.*, (2019) and excellent durability properties Aiken *et al.*, (2018) than Portland Cement Concrete (PCC). SCMs have received extensive attention by researchers that have successfully applied them to the construction of civil engineering infrastructure to replace PC utilization Mark *et al.*, (2019). Production of PC required high amount of energy and emission of about 8% CO_2 to the atmosphere is significant to Green House Gasses (GHG). Consequently, about 85% reduction of CO_2emissions per ton and 58% reduction of energy needs (MJ/ton) were observed during geopolymer binder production compared with PC Davidovits, (1994).

Geopolymers are principally known for their high compressive strength, acid resistance and waste encapsulation capability, though the inorganic framework structure renders these materials intrinsically fire-resistant (Davidovits, 1989; Davidovits, 1991). Geopolymers may be synthesized at ambient or elevated temperature by alkaline activation of a large variety of alumino-silicate materials obtained from industrial wastes (Bakharev *et al.*, 1999; Duxson & Provis, 2008), calcined clays (Duxson *et al.*, 2005; Panagiotopoulou *et al.*, 2007), natural minerals (Chen and Brouwers, 2007), or mixtures of two or more of these materials (BS1881-125,2013; Khale and Chaudhary, 2007).

Response Surface Methodology (RSM) is a statistical and analytical method that examines the effect of a set of quantitative experimental variables of factors on response Myers *et al.*, (2009). RSM is usually employed to identify a set of vital elements (operating conditions) generating the best" response Myers *et al.*, (2009). However, an appropriate Design of Experiment (DOE) can be used to evaluate the effects of these factors with a small number of experiments Onoue & Bier (2017). The ultimate objective is to minimize the required effort and maximize the expected benefit Onoue & Bier (2017). Therefore, the needed action or the desired use in any practical circumstance can be termed as optimization that evaluates a function's conditions, thus minimizing or maximizing the values Onoue & Bier (2017).

The obtained results indicated that the strength value for the materials could be optimized using numerical techniques and the DOE in the response surface method, Onoue & Bier (2017). In the study, while the flexural strength was maximized, the mix proportion properties were minimized. There was a strong correlation between the experimental flexural and optimized flexural strength. However, Ramkumar *et al.*, (2017) in the "Application of response surface methodology for optimization of alkali activated slag concrete", employed the CCD of the RSM to optimize the mechanical strengths of fly ash-based GPC. It was concluded that the RSM validated the influence factors with an average difference of less than 5%, hence acceptable. However, the optimization of metakaolin-based GPC product modified by metabentonite is a novel development as no study has been conducted on optimizing its strength through RSM-2^2 Factorial Design.

In this regard, this paper aims to obtain an optimum mix design and mechanical parameters of metabentonite/metakaolin-based geopolymer concrete using response surface method

(RSM). Therefore, the 2^2 Factorial Design model of RSM was employed to arrive at an optimum combination of mix parameters of metabentonite/metakaolin-based GPC. The selected mix parameters were metabentonite-to-metakaolin ratio, alkaline liquid-to-binder ratio and 12 molar concentrations of NaOH and Na2Si3O/NaOH ratio of 1.5:1, 28 days curing times as mix design proportions. In addition, the characteristic compressive strengths of M 25 concrete grades were selected as the target strengths. The GPC fresh samples were cured under ambient conditions for 24hours, demoulded and then 60^{O}C heat curing conditions for 24 hours. Ultimately, the developed models can be applied to predict the compressive strength of geopolymer concrete incorporating geological clay mineral pozzolans in a building sector, thus reducing cost, energy, and time while conducting laboratory works.

Materials and Methods

Raw Materials

Bentonite and kaolin were locally sourced and used as precursor materials then beneficiated, heated at 105 °C for 24 h to remove the water content. The dried bentonite and kaolin were crushed and grounded (3000 cycles) in a ball mill to increase its fineness as cement (range of 100μm), calcined at 650°C and 700°C for two hours to acquire the metabentonite and metakaolin respectively.

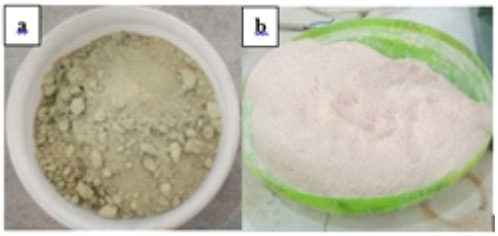

Figure 1: Source materials used: (a) Bentonite and (b) Kaolin.

Therefore, both bentonite and kaolin, as shown in Figure 1, were used as the source materials to produce GPC, while the fine aggregate were source locally and coarse aggregate were source from quarry site and tests were carried out in accordance with BS EN 933-1 and BS EN 12620: (2002). Alkaline were sourced from a chemical supplier. The NaOH was in pellet form and Na_2SiO_3 in form of liquid gel. The Specific Gravity (SG) of the precursor materials was obtained following the BS EN (2016) procedure through kerosene and SG bottle, the results of which are presented in Table 1.

Table 1: Physical properties of the precursor materials used.

Names of property	Metabentonite	Metakaolin
Specific Gravity (g/cm^3)	3.23	2.34
Physical form	Powder	Powder
Colour	Grayish - brown	Baby Pink

The chemical compositions of the metabentonite and metakaolin samples were carried out using X-Ray fluorescence (XRF) analysis (X-supreme 8000) instrument and the result of XRF indicates that chemical composition of the precursor was conforming to BS EN 197-1: (2011) for natural calcined pozzolans (Q). The obtained results are shown in Table 2.

Table 2: Oxide composition of Metabentonite and Metakaolin

Element	Metabentonite Content (%)	Metakaolin Content (%)
Al_2O_3(%)	25.5632	41.9270
SiO_2(%)	51.0558	52.4100
P_2O_5(%)	0.3781	-
SO_3(%)	0.0977	0.1310
K_2O(%)	0.3879	0.5801
CaO(%)	5.4604	0.0840
TiO_2(%)	1.1196	0.0500
MnO(%)	0.0902	0.3780
Fe_2O_3(%)	14.2364	0.9080
NiO(%)	0.0643	-
ZnO(%)	0.0051	0.0011
SrO(%)	0.6289	0.0021
MoO_3(%)	0.0074	-
PdO(%)	0.0181	-
Ag_2O(%)	0.0043	-
Sb_2O_5(%)	0.0023	-
BaO(%)	0.8480	-
PbO(%)	0.0116	0.0020
Na_2O(%)	-	0.2890
MgO**(%)**	-	0.4302
SrO**(%)**	0.6289	-

Source: Laboratory work (2021)

Table 3: Comparison of oxide composition

Precursor	Oxides	Value	ASTMC618-05	Getso A. I (2013)
Metabentonite	Al2O3+SiO2 + Fe2O3	90.8554%	≥70%	
Metakaolin	Al2O3+SiO2 + Fe2O3	95.2450%	≥70%	94.90%
Average	CaO + MgO	3.051%	≤ 5%	0.29%

480 g of NaOH pellets were measured and dissolved in 1ltr of clean water to prepare 12 M activator using $Na_2SiO_3$to NaOH solutions with a ratio of 1.5:1. The activator and proportion were selected in compliance with those of other relevant studies Oyebisi et al., (2020)

Response Surface Method (RSM)

Randomized Block Factorial Design

The Randomized Block2^2 Factorial Design of RSM were employed to evaluate the interaction between the selected continuous variables (A; metabentonite to metakaolin ratio and B; alkaline liquid to binder ratio) and response variable, compressive strength (MPa). Design

expert 13 statistical software was engaged, and the 2^2 Factorial Design was created using two different continuous variables, the results of which are shown in table 4.

Table 4: Factors

Factor	Name	Level	Low Level	High Level	Std. Dev.	Coding
A	Metabent	37.89	10.00	50.00	0.0000	Actual
B	Alkali Doss	78.32	50.00	90.00	0.0000	Actual

In the study, 2^2 Factorial Design were considered to test two factors A (metabentonite) and B (Alkali doss) each measured in percentage. If A has (a = 5; 10, 20, 30, 40, and 50) levels and B has (b = 5; 50, 60, 70, 80, 90) levels, each complete replicate of the experiment will contain (a x b = 5 x 5 = 25) runs (or treatment combinations).

Table 5: Concrete mix proportions for cube samples

S/N	Metabentonite (%)	Alkali (%)	Metabent. (kg/m^3)	Metakaolin (kg/m^3)	Fine Agg. (kg/m^3)	Coarse Agg. (kg/m^3)	Alkali (kg/m^3)
1	40	50	240	360	600	1200	300
2	10	50	60	540	600	1200	300
3	10	80	60	540	600	1200	480
4	50	80	300	300	600	1200	480
5	30	60	180	420	600	1200	360
6	50	60	300	300	600	1200	360
7	10	90	60	540	600	1200	540
8	30	90	180	420	600	1200	540
9	40	90	240	360	600	1200	540
10	50	70	300	300	600	1200	420
11	40	80	240	360	600	1200	480
12	40	70	240	360	600	1200	420
13	20	50	120	480	600	1200	300
14	30	80	180	420	600	1200	480
15	20	80	120	480	600	1200	480
16	20	90	120	480	600	1200	540
17	10	70	60	540	600	1200	420
18	20	70	120	480	600	1200	420
19	30	50	180	420	600	1200	300
20	10	60	60	540	600	1200	360
21	40	60	240	360	600	1200	360
22	20	60	120	480	600	1200	360
23	30	70	180	420	600	1200	420
24	50	90	300	300	600	1200	540
25	50	50	300	300	600	1200	300

Development of Mathematical Model

In RSM, the standard factorial in a randomized block design, choosing a model type depends on the nature of accessible information and levels for each factor. For the most part, for an experiment matrix that has been as of now built up, the historical data or user-defined model was applied for the development and investigation of a model Kumar & Baskar, (2014).

The polynomial equation of the correlation between the response variables and independent variables can be expressed in a general form as follows (Kumar & Baskar, (2014).)

$$Y = \beta_0 + \Sigma_{i=1}^{k}\beta_i X_i + \Sigma_{i=1}^{k}\beta_{ii}X_{ii}^2 + \Sigma_{j=2}^{k}\Sigma_{i\leq i\leq j}^{j=1}\beta_{ij}X_iX_j + \varepsilon \qquad (1)$$

Where Y is the response, xi and xj are the independent variables (i and j are the range from 1 to k), β_o is the constant coefficient, β_i, β_{ii} and β_{ij} are the coefficient for the linear, quadratic and interaction effect, and ε represent the error. Sum of squares, F value, probability (P-value) with 95 % confidence level and coefficient of correlation (R^2), ranging from 0 to 1 was employed to predict the fitness or measure the quality of the developed model. A highly significant and accurate model is indicated by R^2 close to 1.

Optimization: The Desirability Approach

The desirability function approach is one of the most widely used methods in industry for the Optimization of response surface processes. It is based on the idea that the "quality" of a product or process that has multiple quality characteristics, with one of them outside of some "desired" limits, is completely unacceptable. The method finds operating conditions ***x*** that provide the "most desirable" response values.

For each response ***Yi*(*x*)**, a desirability function ***di*(*Yi*)** assigns numbers between 0 and 1 to the possible values of ***Yi***, with ***di*(*Yi*) = 0** representing a completely undesirable value of ***Yi*** and ***di*(*Yi*) = 1** representing a completely desirable or ideal response value. The individual desirabilities are then combined using the geometric mean, which gives the overall desirability D:

$$\mathbf{D} = (d_1(Y_1) \times d_2(Y_2) \times \ldots \times d_k(Y_k))^{1/k} \qquad (2)$$

With **k** denoting the number of responses. Notice that if any response ***Yi*** is completely undesirable **(*di*(*Yi*) = 0)**, then the overall desirability is zero. In practice, fitted response values ***i***are used in place of the ***Yi***.

Depending on whether a particular response ***Yi*** is to be maximized, minimized, or assigned a target value, different desirability functions ***di*(*Yi*)** can be used. A useful class of desirability functions was proposed by (Derringer and Suich1980; Myers, *et al.*, 2009). Let ***Li*, *Ui*** and ***Ti***be the lower, upper, and target values, respectively, that are desired for response ***Yi***, with ***Li* ≤ *Ti* ≤ *Ui***.

If a response is of the "target is best" kind, then its individual desirability function is with the exponents ***s*** and ***t*** determining how important it is to hit the target value Myers, *et al.*, (2009). For ***s* = *t* = 1**, the desirability function increases linearly towards ***Ti***; for ***s* < 1, *t* < 1**, the function is convex, and for***s*> 1, *t* > 1**, the function is concave.

$$d_i(\hat{Y}_i) = \begin{cases} 0 & \text{if } \hat{Y}_i(x) < L_i \\ \left(\frac{\hat{Y}_i(x)-L_i}{T_i-L_i}\right)^s & \text{if } L_i \le \hat{Y}_i(x) \le T_i \\ \left(\frac{\hat{Y}_i(x)-U_i}{T_i-U_i}\right)^t & \text{if } T_i \le \hat{Y}_i(x) \le U_i \\ 0 & \text{if } \hat{Y}_i(x) > U_i \end{cases} \quad (3)$$

If a response is to be maximized instead, the individual desirability is defined as with

$$d_i(\hat{Y}_i) = \begin{cases} 0 & \text{if } \hat{Y}_i(x) < L_i \\ \left(\frac{\hat{Y}_i(x)-L_i}{T_i-L_i}\right)^s & \text{if } L_i \le \hat{Y}_i(x) \le T_i \\ 1.0 & \text{if } \hat{Y}_i(x) > T_i \end{cases} \quad (5)$$

The desirability approach consists of the following steps:

i. Conduct experiments and fit response models for all **k** responses;
ii. Define individual desirability functions for each response;
iii. Maximize the overall desirability ***D*** with respect to the controllable factors.

Mixing Procedure for Geopolymer Concrete

The mixing method of geopolymer concrete was performed by adopting the traditional techniques used in the production of normal concrete (Rangan. 2011). Firstly, all materials; metabentonite, metakaolin, fine aggregate, and coarse aggregate were mixed in a dry condition in the concrete mixer for approximately three minutes. The alkaline solution was mixed for approximately two minutes. After that, the alkali liquid activator components were added to the dry materials and the mixing was continued for 7 minutes for uniform mixing. The mixing was continued for further 3 minutes and the GPC were poured into pre-oiled mould (Rangan. 2011). The fresh GPC was compacted by using vibrating table and casted into the cube specimens of size 100mm X100mm X 100mm, demoulded after 24h and oven heat under constant curing temperature of 60°C for 24h and curing duration of 28d under room temperature. The alkaline activator-to-binder ratio was varied at 50%, 60%, 70%, 80%, and 90% and the metabentonite-to-metakaolin ratio was 10%, 20% 30%, 40% and 50% with solution molar concentrations of 12M and Na_2SiO_3/NaOH ratio of 1.5:1.

Test Methods

The data to be followed in the developed models using RSM for optimization were evaluated from the laboratory analysis. To evaluate the mutual correlation with the variables, compressive strength at 28 days as hardened properties of geopolymer concrete were taken as the response of interest.

The characterizations of the used source materials were analyzed using Fourier Transform Infrared (FTIR) Spectroscopy carried out using FTIR (Cary 630 Agilent Technology USA equipment). All FT-IR spectra were recorded in the range of 4000–400 cm^{-1} at a resolution of 4 cm^{-}

Result and Discussion

Response Surface Optimization

The experimental trials were made by the suggested DOE input from RSM. The resulted compressive strength of various mixes has been made as a step for further analysis.

Analysis of Variance

Following the creation of randomized block factorial design and establishment of response surface design from data in a worksheet, as illustrated in Table 4, the fitted model analysis results for a response surface design are presented in Table 6. The model's accuracy and the influence of continuous variables on the compressive strength were examined by analyzing variance (ANOVA).

The regression model in Table 6 indicates that the terms in the model have a significant effect on the compressive strength because p-value<0.0001, which is less than -level (0.05) Asadzadeh and Khoshbayan (2018). Consequently, the p-values for the continuous variables, A and B are <0.0001 and 0.0006 respectively, indicating the significant linear effect. The resisting performance of the concrete against compressive failure depends on the proportions of alkaline liquid and binder.

The terms AB^3, were regarded as non-significant terms and removed from the model according to the P-value. Therefore, according to Table 6, the P-values of 0.1475, and 0.1481for the squared and cubic effects, B^2 and B^3 respectively, were higher than 0.05, indicating that the relationship between compressive strength and B exhibited no significant quadratic effect. However, the p-values of<0.0001 each for the AB, A^2, AB^2, A^2B, A^3, A^2B^2, A^3B, A^4 andB^4 respectively, were less than 0.05, indicating a significant interaction effect. The effect of A on the resisting performance of concrete against failure depends on B. However, as shown in Table 6, the F-value for all significant terms was greater than 5, confirming that the model terms were substantial Oyebisi et al., (2020) to the yield of compressive strength. Finally, the model yielded no lack of fit or pure error because both linear and interaction terms were significant, hence included in the model.

Table 6: ANOVA for Compressive strength, CP12M1.5

Source	Sum of Squares	df	Mean Square	F-value	p-value
Model	479.48	13	36.88	288.97	< 0.0001
A-Metabent	43.12	1	43.12	337.84	< 0.0001
B-Alkali Doss	1.58	1	1.58	12.41	0.0006
AB	19.74	1	19.74	154.66	< 0.0001
A^2	35.17	1	35.17	275.57	< 0.0001
B^2	0.2708	1	0.2708	2.12	0.1475
A^2B	9.26	1	9.26	72.56	< 0.0001
AB^2	9.77	1	9.77	76.56	< 0.0001
A^3	17.57	1	17.57	137.65	< 0.0001
B^3	0.2700	1	0.2700	2.12	0.1481
A^2B^2	5.58	1	5.58	43.71	< 0.0001
A^3B	10.45	1	10.45	81.91	< 0.0001
A^4	20.64	1	20.64	161.72	< 0.0001
B^4	2.19	1	2.19	17.15	< 0.0001
Residual	17.36	136	0.1276		
Pure Error	0.0000	125	0.0000		
Cor Total	496.84	149			

The model summary yielded R^2, R^2(adj), and R^2 (pred) as 96.51%, 96.15%, and 95.82%, respectively, showing that the model equation could predict the relationship between the response variable and continuous variables at 100% confidence bound. Ultimately, this developed model equation can be used to predict the compression optimization of the metakaolin-based GP concrete strength incorporated with metabentonite.

$$\textbf{CP12M1.5} = 25.4 - 2.45A - 0.47B + 2.18AB - 6.96A^2 + 0.6077B^2 + 0.84A^2B - 0.8629AB^2 + 1.61A^3 + 0.2B^3 - 1.1A^2B^2 - 1.76A^3B + 4.63A^4 - 1.51B^4 \quad (6)$$

Diagnostic plots are useful to see whether assumptions are met. Fig 2, shows the residual plot diagram exhibiting the fits and the experimental observation for the attribute, the compressive strength.

In practice, a balanced or nearly balanced design wi tha large number of observations does not significantly affect the residuals (the difference between the observed and fitted response variables) if departed moderately from a straight line or normality Myers *et al.* (2009). Hence, the normally distributed residual from the analysis is required for a balanced design. As shown in Figure 2, the residuals generally follow a straight-line pattern, hence no evidence of non-normality or unknown variables in the model. As observed, there is no significant defection

from the normal probability line and can be fairly conclude that the assumption of normality is satisfied. Furthermore, in a designed experiment, the order of observations affects the response variable if the residuals fluctuate in a random pattern around the center line Myers *et al.,* (2009). The result versus order for the response variable, as shown in Figure 3, exhibited a randomly scattered pattern about zero, hence no evidence of the correlation among the error terms.

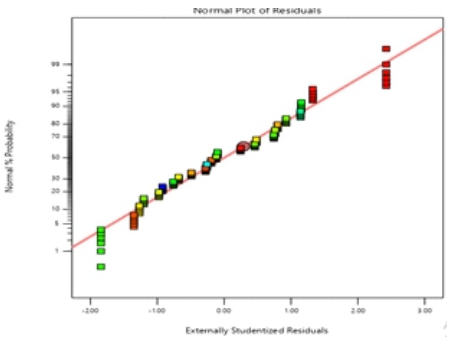

Figure 2: Normal probability plot of Cr (MPa).

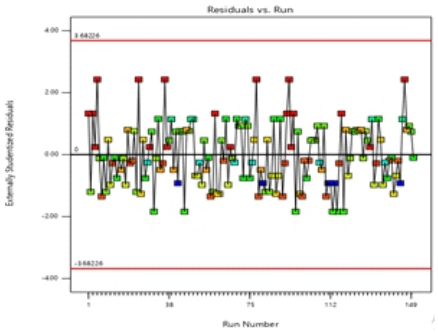

Figure 3: Residual versus order plot**.**

Establishment of desirable response value and operating conditions

Operating conditions of B and A on the compressive strength

Figure 4 shows the compressive strength with the binder ratio (metabentonite substitute (%)) and alkaline liquid-to-binder proportions (%) following the model equation. BothNa_2Si_3O/NaOH ratio of 1.5:1 and curing time were kept constant. Figure 4 illustrates the visualized effect of both B and A on both 2D contour lines of the binder.

According to Figure 4, the optimum compressive strength of 26.1722 (MPa) was attributed to the lower metabentonite of about 24.9558% and alkaline dosage of 56.9628 % at a constantNa2Si3O/NaOH ratio on 28 days curing period.

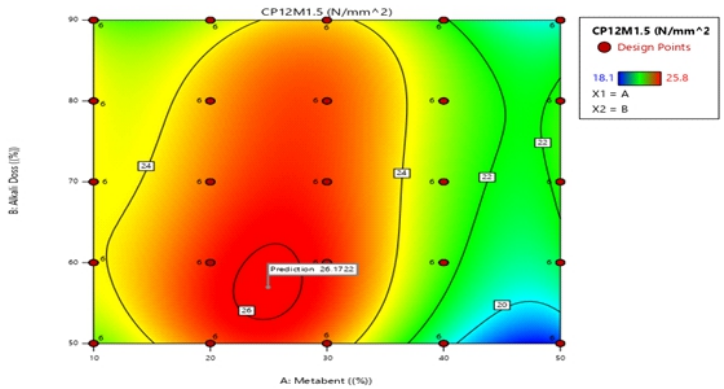

Figure 4: Interaction between B and A on the maximized compressive strength (MPa).

However, any change in the contours values alters the color and shape patterns of the continuous variables. As shown in Figure 5, the red area indicates the contour, which yields the highest compressive strength (26.1722 MPa). Therefore, the resistance of the GP concrete product against compression under the applied load can be optimized at target compressive strength of 25 MPa with the corresponding continuous variables of around 25% and 84% for A and B respectively.

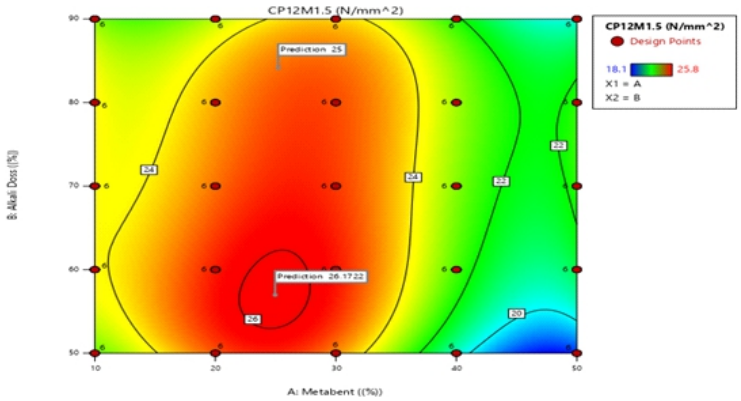

Figure 5: Interaction between B and A on the target compressive strength (25 MPa).

Relationship between experimental and Optimized Compressive Strengths

Through the fitted linear regression equation, the relationship between the optimized compressive strength and experimental compressive strength is given in Figure 7. The results indicated that there was a strong correlation between the optimized compressive and experimental compressive strength. The coefficient of determination (R^2) also demonstrated that the model was 96.51% it to predicting the relationship between optimized compressive and experimental compressive strength at both 95% confidence and predictive intervals. Furthermore, the standard distance (S) of the response demonstrated that the data values were concentrated on the regression line; hence, the data values fitted the regression line, and the model equation could significantly predict the response Oyebisi *et al.,* (2021).

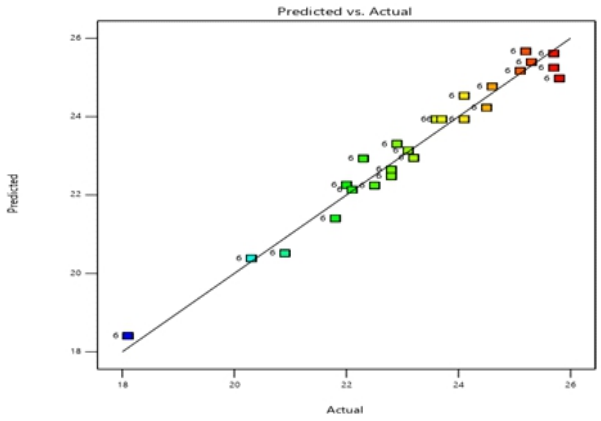

Figure 7: Relationship between Optimized and Experimental CP12M1.5.

FTIR Analysis

The FTIR spectra of Metabentonite and Metakaolin Blended GPC are shown in Fig. 8. Similar trends in the FTIR spectra, with a broad band around 3265 cm^{-1} can be attributed to the -OH stretching vibration Ji & Pei, (2020), and the broadband around 1640 cm^{-1} can be attributed to the H-O-H bending vibration Opiso *et al.*, (2021)., which is due to the adsorption of H_2O molecules on the surface of the geopolymer and in the internal cavities Xia *et al.,*(2019). The strong absorption peak in the broad band around 1397 $cm^{-1}$and 872 cm^{-1} are caused by the stretching vibration of the O-C-O bond in carbonates Jin *et al.*, (2016), indicating the reaction of Ca $(OH)_2$ and CO_2 to form $CaCO_3$ or the presence of unreacted carbonates. The broad band around 984 cm^{-1} can be assigned to the asymmetric stretching vibration due to Si-O-X (X = Si or Al), and these bonds are geopolymer gel formed as the result of activation, indicating that Metabentonite and Metakaolin Blended GPC were successfully synthesized (Ji & Pei, 2019: Liew *et al.*, 2012). It should be noted that Metabentonite and Metakaolin Blended GPC has a strong absorption peak indicating a higher degree of geopolymerization, which provides support for the high compressive strength and immobilization efficiency. Moreover, some studies have also shown that Si-O-Si or Si-O-Al may shift to nonbridging oxygen (Si-O-Na+, Al-O-Na+) resulted from the reaction of alumino-silicates with alkali, and that Pb^{2+} can undergo ion exchange with Ca^{2+} or Na^{+}(El-Eswed *et al.*, 2017:. Zhao *et al.*, 2019). The broad band around 711.9 cm^{-1} is caused by the symmetric stretching vibration of Si-O-Al and Al-O-Si Park et al., (2018).

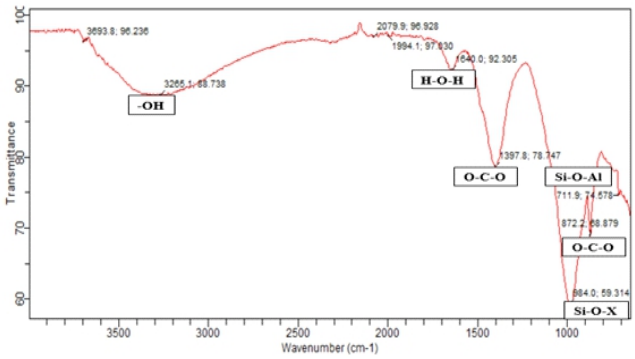

Figure 8: FTIR Spectra of Metabentonite and Metakaolin Blended GPC

Conclusions

This work evaluated the compressive strength of the metakaolin-based GPC modified by metabentonite. The metabentonite incorporated results were compared with those of the control samples metakaolin-based GPC. In this study, while the compressive strength was maximized, the mix proportion properties were in range. Therefore, the following conclusions were made:

1. A geopolymer concrete has been successfully produced by using bentonite and kaolin. The DOE of randomized block factorial design was performed using RSM and mathematical model was developed. Its characterization using FTIR showed that the alumino-silicate structure was formed in all prepared samples.
2. The compressive strength CP12M1.5 of metabentonite-metakaolin based geopolymer are directly proportional to the metabentonite substitution and alkali doss

percentage. CP12M1.5 showed maximum compressive strength due to effects of combined variables.

3. However, the effects of combined variables have been studied and optimized using the RSM technique. Geopolymer concrete with approximately 25 %metabentonite and 57 % alkaline dosage exhibits maximum compressive strength CP12M1.5 of 26 N/mm^2 and optimum proportion of 25 % metabentonite and 84 % alkaline dosage was exhibited at target compressive strengthCP12M1.5 of 25 N/mm^2at 28days constant curing periods.
4. Based on optimization studies, the coefficient of correlation (R^2) obtained was 96.51% at the optimum formulation (desirability value = 90.47%).

Reference

Aiken, T. A., Kwasny, J., Sha, W., & Soutsos, M. N. (2018). Effect of slag content and activator dosage on the resistance of fly ash geopolymer binders to sulfuric acid attack, *Cement and Concrete Research, 111*, 23-40.

Asadzadeh, S. & Khoshbayan, S. (2018). "Multi-objective optimization of influential factors on the production process of foamed concrete using Box-Behnken approach, *Construction and Building Materials*, *170*, 101-110

Bakharev, T. Sanjayan, J. G, & Cheng, Y. B, (1999). Alkali activation of Australian slag cements, *Cement and Concrete Research 29* (1), 13-120

Bouaissi, A., Li, L., Abdullah, M., & Bui, Q. (2019). Mechanical properties and microstructure analysis of FA-GGBS-HMN based geopolymer concrete, *Construction and Building Materials*, *210*, 198-209.

British Standard 1881-125, (2013). *Testing concrete: Methods for mixing and sampling fresh concrete in the laboratory*, BSI, London

British Standard EN 196-3, (2016). *Method of testing cement: Physical test*, BSI, London.

Chen, W. & Brouwers, H. (2007). The hydration of slag, Part 1: Reaction models for alkali-activated slag, *Journal of Materials Science*, *42*, 428-443.

Davidovits, J, (1989). Geopolymers and geopolymeric materials, *Journal of Thermal Analysis 35,* 429-441

Davidovits J, (1991). Geopolymers inorganic polymeric new materials, *Journal of Thermal Analysis 37*, 1633-1656

Davidovits, J. (1994). *High-alkali cement for 21st century concretes", in Concrete Technology*, Past, Present and Future, Proceedings of V, Mohan Malhotra Symposium, American Concrete Institute, 144, 383-397

Derringer, G. & Suich, R. (1980). Simultaneous optimization of several response variables, *Journal of Quality Technology*, *12*, 214-219

Duxson P, & Provis, J. L, (2008). Designing precursors for geopolymer cements, *Journal of the American Ceramic Society 91*, 3864-3869

Duxson, P, Provis, J. L, Lukey, G. C, Mallicoat, S. W, Kriven W. M, & Van-Deventer, J. S. J. (2005). Understanding the relationship between geopolymer composition, microstructure And mechanical properties, *Colloids and Surfaces A: Physicochem Engineering Aspects 269,* 47-58

El-Eswed, B. I, Aldagag, O. M., & Khalili, F. I., (2017). Efficiency and mechanism of stabilization/ solidification of Pb(II), Cd(II), Cu(II), Th(IV) and U(VI) in metakaolin based geopolymers, *Applied Clay Science, 140,* 148-156.

Ji, Z. & Pei, Y. (2019). Geopolymers produced from drinking water treatment residue and bottom ash for the immobilization of heavy metals, *Chemosphere*, *225*, 579-587.

Ji, Z. & Pei, Y., (2020). Immobilization efficiency and mechanism of metal cations (Cd2+, Pb2+ and Zn2+) and anions (AsO43- and Cr2O72-) in wastes-based geopolymer, *Journal of Hazardous Materials*, *384*, 121290

Jin, M., Zheng, Z., Sun, Y., Chen, L., & Jin, Z. (2016). Resistance of metakaolin-MSWI fly ash based Geopolymer to acid and alkaline environments, *Journal of Non-Crystalline Solids*, *450,* 116-122.

Khale, D. & Chaudhary, R. (2007). Mechanism of geopolymerization and factors influencing its development: A review, *Journal of Materials Science, 42,* 729-749

Liew, Y. M., Kamarudin, H., Mustafa, A., Bakri, A. M., Bnhussain, M., Luqman, M., Khairul, N. I., Ruzaidi, C. M., & Heah, C. Y., (2012). Optimization of solids-to-liquid and alkali activator ratios of calcined kaolin geopolymeric powder, *Construction and Building Materials*, *37*, 440-451.

Mark, O. G., Ede, A. N., Olofinnade, O., Bamigboye, G., Okeke, C., Oyebisi, S. O., & Arum, C. (2019). Influence of some selected supplementary cementitious materials on workability and compressive strength of concrete a review, *IOP Conference Series: Materials Science and Engineering, 640*, 012-071

Myers, R. H., Montgomery, D. C., & Anderson-Cook, C. M., (2009*). Response surface methodology: Process and product optimization using designed of experiments, 3rd edition*, John Wiley and Sons, Inc. New Jersey.

Onoue, K. & Bier, T. A. (2017). Optimization of alkali activated mortar utilizing ground granulated blast furnace slag and natural pozzolan from Germany with the dynamic approach of the Taguchi method, *Construction and Building Materials*, 144, 357-372

Opiso, E. M., Tabelin, C. B., Maestre, C. V., Aseniero, J. P. J., & ParkI. M, (2021). Villacorte-Tabelin, synthesis and characterization of coal fly ash and palm oil fuel ash modified artisanal and small-scale gold mine (ASGM) tailings based geopolymer using sugar mill lime sludge as Ca-based activator, Heliyon, 7 e06654.

Oyebisi, S., Ede, A., Olutoge, F., & Omole, D. (2020). Geopolymer concrete incorporating agro-industrial wastes: Effects on mechanical properties, Microstructural behaviour and mineralogical phases*, Construction and Building Materials*, 256, 119390.

Oyebisi, S., Ede, A., Olutoge, F., & Olukanni, D. (2020). Assessment of activity moduli and acidic resistance of slag-based geopolymer concrete incorporating pozzolan, *Case Studies in Construction Materials,* 13, e0039456.

Oyebisi, S. O., Ede, A. N., & Olutoge, F. A. (2021). Optimization of design parameters of slag-corncob ash-based geopolymer concrete by the central composite design of the response surface methodology, *Iranian Journal of Science and Technology, Transactions of Civil Engineering*, *45*(1), 2742

Panagiotopoulou, C, Kontori, E, Perraki, T, & Kakali, G, (2007). Dissolution of alumino-silicate minerals and by-products in alkaline media, *Journal of Material Science 42,* 2967-2973

Ramkumar, B. G., Barmavath, S., & Nagaraju, K. (2017). Application of response surface methodology for optimization of alkali activated slag concrete, *International Journal of Science, Development and Research*, *2*(3), 35- 47.

Rangan. B. V. (2011). Fly ash based geopolymer concrete, *proceeding of International Workshop on Geopolymer cement and Concrete, Mumbai, India, December*, 68-106

Senthil-Kumar, K., & Baskar, K., (2014). Response surfaces for fresh and hardened properties of concrete with e-waste (HIPS), J. Waste Manag.

Park I., Tabelin, C. B., Seno, K., Jeon, S., & Ito, M. N., (2018). Hiroyoshi, simultaneous suppression of acid mine drainage formation and arsenic release by Carrier-microencapsulation using aluminum-catecholate complexes, Chemosphere, *205*, 414-425.

Xia, M., Muhammad, F., Zeng, L., Li, S., Huang, X., Jiao, B., Shiau, Y., & Li, D., (2019). Solidification/ Stabilization of lead-zinc smelting slag in composite based geopolymer, *Journal of Cleaner Production*, *209*, 206-1215.

Zhao, S., Muhammad, F., Yu, L., Xia, M., Huang, X., Jiao, B., Lu, N., & Li, D., (2019). Solidification/ stabilization of municipal solid waste incineration fly ash using uncalcined coal gangue–based alkali-activated cementitious materials, *Environmental Science and Pollution Research, 26*, 25609-25620.